Mixed-Species Targets for Femtosecond-Time-Scale X-Ray Generation

S. E. Harris and J. D. Kmetec
Edward L. Ginzton Laboratory, Stanford University, Stanford, California 94305
(Received 16 February 1988)

We suggest the use of mixtures of light and heavy elements as targets for laser-driven femtosecond-time-scale x-ray line radiators. It is shown that the essential cooling of a heavy metal together with the loss-modified thermal conductivity allows an x-ray pulse to replicate a laser pulse on a femtosecond time scale, and to achieve such an x-ray pulse, the density of heavy metal must be reduced to a level commensurate with the absorbed laser energy. Results of numerical modeling for the generation of 3.6-Å x rays in a mixture of Li and Sn are given.

PACS numbers: 42.65.Re, 32.30.Rj, 52.25.Nr, 52.50.Jm

This Letter suggests the use of mixtures of light and heavy elements as targets for laser-driven femtosecond-time-scale x-ray line radiators. We illustrate with a mixture of lithium (Li) doped with several percent tin (Sn). We assume that a tightly focused 100-fs laser pulse is incident on the surface of a mixed-species target and that some fraction of the laser energy is absorbed in a skin depth of about 150 Å. Electrons in the interior (about 10^4 Å) of the metal are heated by electron-electron diffusive energy transfer and are cooled by ionizing collisions with heavy-metal atoms, and also, to some extent, by thermal diffusion further into the interior. Electrons make inner-shell holes in heavy-metal target atoms, which in turn radiate. The preponderance of light metal allows a much higher electron temperature, and therefore, at a given absorbed laser energy density, a conversion efficiency to x rays which can be much larger than for a solid-density heavy metal alone.

Though the radiation from the target species will result from all core transitions, it is advantageous to adjust the electron temperature so that an L-M transition is dominantly excited. The reason for this is that the Auger decay rate of the M shell is most often determined by Coster-Kronig decay,[1] and is generally as fast as, or faster than, the Auger rate of the L shell.[2] This raises the effective radiation temperature, and also, by increasing the lower-level linewidth, reduces the absorption cross section of M-shell ions thereby preventing radiative trapping of the generated x rays. The L-M transition wavelength for Sn is 3.6 Å; the L-shell radiative rate is $2.5\times10^{14}\ s^{-1}$; the L-shell Auger rate is $3\times10^{15}\ s^{-1}$; and the M-shell Auger rate is $4\times10^{15}\ s^{-1}$.

Before proceeding, we note that there have been suggestions[3] and first experiments[4-7] for using picosecond- and femtosecond-time-scale lasers to drive x-ray-emitting plasmas. Also, there are some measurements which show x-ray pulse lengthening well into the picosecond range.[8] But these experiments have operated very differently from that postulated here. Both because of the lower power density on target, and because the targets were heavy metals, the electron temperatures were low; and the rise and fall times of the x-ray pulse were dominated by avalanche stripdown and by two-body radiative recombination. These are inherently much slower than are the electron heating and cooling times described herein.

The partial differential equations which relate the heat flux q, the electron temperature T, and the electron density n_e are

$$\frac{\partial q}{\partial x} = -\frac{3}{2}n_e\frac{\partial}{\partial t}(kT) - n_e\frac{\partial \mathcal{E}_L}{\partial t} + U(x,t), \tag{1a}$$

$$\partial T/\partial x = -\kappa^{-1}q, \tag{1b}$$

$$\partial n_e/\partial t = \left(\textstyle\sum_j \langle\sigma v\rangle_j \langle Z_j\rangle\right) n_e, \tag{1c}$$

where each of the variables and also κ and $\langle\sigma v\rangle_j$ are functions of space and time. In these equations, κ is the mixed-species thermal conductivity, $\partial\mathcal{E}_L/\partial t$ is the energy loss per electron which results from inelastic collisions of the electrons with atoms and ions, and $U(x,t)$ is the laser driving term. The quantity $\sum_j\langle\sigma v\rangle_j\langle Z_j\rangle$ is the velocity-averaged, time- and space-dependent electron ionization rate, and is summed over all bound electrons j of all atoms and ions. $\langle Z_j\rangle$ is the average number of cascade Auger electrons which are produced following the ionization of the jth bound electron. For the temperatures and time scale discussed here, both hydrodynamic expansion of the target and electron-ion recombination can be neglected.

Since the time scale of the proposed experiment (100 fs) is in the range of the temperature-dependent electron energy thermalization time[9] ($\simeq$1-25 fs), the extent to which the secondary and Auger electrons thermalize with the primary electrons is not clear. For no thermalization, the primary electrons lose energy according to the Maxwellian-averaged Bethe formula,[10]

$$\left(\frac{\partial\mathcal{E}_L}{\partial t}\right)_B = 4\pi^2e^4\bar{g}\left(\frac{2}{3\pi kTm}\right)^{1/2}\sum_j \exp\left(-\frac{E_j}{kT}\right), \tag{2a}$$

where e and m are the charge and mass, and E_j is the binding energy of the jth electron. An average effective Gaunt factor $\bar{g}=0.3$ is used.

For this work we assume a Maxwellian electron temperature distribution, and therefore employ a specific heat model.[11] Here, the cascade electrons instantly thermalize to temperature T, and Eq. (2a) is replaced by

$$\partial \mathcal{E}_L/\partial t = 4\pi^2 e^4 \bar{g}(2/3\pi kTm)^{1/2} \sum_j E_j^{-1}[\Delta E_j + \tfrac{3}{2} kT\langle Z_j\rangle]\exp(-E_j/kT). \tag{2b}$$

ΔE_j is the total potential energy[12] which is stored in ionic form following the Auger cascade of an ejected electron with threshold E_j. The quantity $\langle Z_j\rangle$ is calculated according to the empirical rules given by Carlson, Hunt, and Krause.[13]

The inelastic energy loss which the electrons experience as a result of ionizing collisions with atoms and ions also affects the thermal conductivity of the mixed-species system. For an ideal gas-kinetic model κ may be shown to be

$$\kappa = \frac{n_e m}{6}\int_0^\infty v^2 \nu_c(v)\left[\frac{\partial N(v,T)}{\partial T}\right]\left[\frac{\lambda(v)\mu(v)}{\mu(v)+\lambda(v)}\right]^2 dv, \tag{3}$$

where $\lambda(v)$ and $\mu(v)$ are the elastic mean free path and $(1/e)$ inelastic stopping distance for an electron of velocity v. The quantities ν_c and $N(v,T)$ are the electron elastic-scattering frequency (usually dominated by ions) and the normalized velocity distribution function. Equation (3) contains the implicit assumptions (1) that inelastic collisions do not deflect the electrons, and (2) that electrons are thermalized until the point of their last elastic-scattering event, and then lose energy exponentially as they move ballistically toward a surface of temperature T. In the limit of no inelastic collisions $\mu(v)\to\infty$, and κ of Eq. (3) reduces to the Spitzer-Härm[9] thermal conductivity. The contribution of a particular atom and ion to the elastic and inelastic mean free path of an electron of energy $\mathcal{E}$ is approximately in the ratio of the number of bound electrons which have an ionization potential less than $\mathcal{E}$ to the square of the charge state of the ion. Therefore, for a 1-keV electron in Sn, the inelastic contribution is only important for charge states less than about eight.

In evaluating Eq. (3), we clamp the maximum energy carried by any velocity class dv to its free-flow value. For 20% Sn in Li at 300 eV, and at the steepest part of the temperature gradient (Fig. 2), clamping is required for energies above about 3 times that of the peak of the electron distribution. This results in a maximum heat flux which is 44% of the Spitzer-Härm value and 35% of the free-flow value.

Equations (1)–(3) are solved with the boundary condition $T=300$ K and $n_e=4\times10^{22}$ electrons/cm^3 (metallic Li) for all x at $t=-\infty$, and subject to a laser power-density deposition function $U(x,t)$ which is Gaussian in time and which damps exponentially with distance,

$$U(x,t) = \left(\frac{4\ln 2}{\pi}\right)^{1/2}\frac{U_0}{\tau d}\exp\left(-\frac{x}{d}\right)\exp\left\{-4\ln 2\left(\frac{t}{\tau}\right)^2\right\}. \tag{4}$$

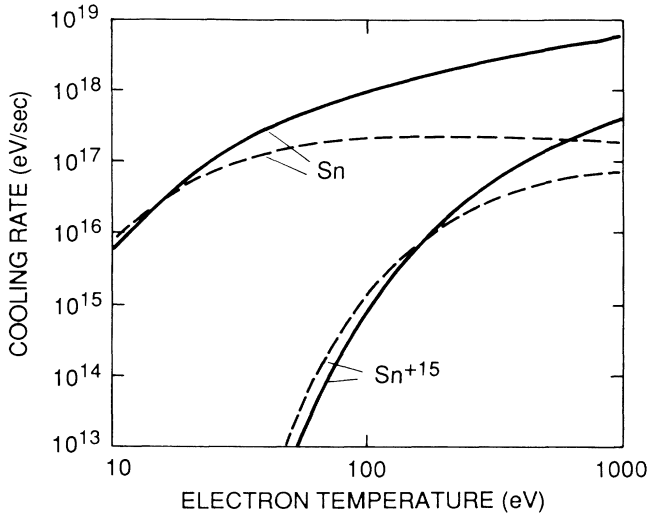

FIG. 1. Electron cooling rates for Sn and Sn^{+15} at solid density as functions of electron temperature. The dashed and solid curves give the results of Eqs. (2a) and (2b), respectively.

Here, U_0 is the total absorbed laser energy per unit of surface area, d is the laser damping length (150 Å), and τ is the laser pulse width (100 fs).

We calculate the x radiation from all L-M transitions, irrespective of the stage of ionization. The rapid Auger decay ($\simeq 4\times10^{15}$ s^{-1}) for Sn prevents radiative trapping, and the x-ray power is calculated by

$$\frac{P}{A}(t) = \hbar\omega\eta \sum_{\substack{L\text{ shell}\\ \text{elec.}}}\int_0^\infty n_e(x)\langle\sigma_L(x,t)v(x,t)x\rangle_j\, dx, \tag{5}$$

where η is the radiative yield (8% for Sn) and $n_e\langle\sigma_L v\rangle_j$ is the (per bound electron) L-shell ionization rate.

In the following paragraphs we give the results of the numerical evaluation of the previous equations. Figure 1 shows the electron energy-loss rate for pure Sn for both the Bethe formula Eq. (2a) and the specific heat formula Eq. (2b), as a function of electron temperature. Since the target will ionize, we also show the electron energy-loss rate for (arbitrarily chosen) Sn^{+15}. Thus, a 1-keV

electron in Sn^{+15} loses energy at a rate of 5×10^{17} eV/s (specific heat model). To heat an electron to 1 keV in 10^{-13} s in the absence of inelastic loss requires (*a priori*) a heating rate of 10^{16} eV/s; this is about 50 times smaller than the pure Sn^{+15} cooling rate.

Figure 2 shows the electron temperature profile as a function of distance for an absorbed energy of 1 kJ/cm^2 at a time of 50 fs after the peak of the laser pulse. At zero Sn density the profile approaches that of Caruso and Gratton[14] for impulsively driven (elastic) diffusive heating. In this limit T varies as the absorbed energy $U_0^{4/9}$.

Figure 3(a) shows the conversion efficiency (absolute) from peak *absorbed* laser power to peak 3.6-Å x-ray power as a function of atomic percent Sn, at several absorbed energy densities. It is seen that the relative advantage of the mixed system, as compared to a pure target, depends on the absorbed laser energy. At 2 kJ/cm^2 a peak power conversion efficiency of about 1.5×10^{-4} occurs at 15% Sn.

Figure 3(b) shows the x-ray pulse length. At very low Sn density the pulse length is primarily controlled by the thermal conductivity. Above a Sn density of about 5%, the x-ray pulse length is controlled by electron cooling [Eq. (2b)], and is as short as or shorter than the applied laser pulse.

We estimate that the two-body recombination radiation within a 20-eV bandwidth centered at 3.6 Å and integrated over all time is a factor of 10^2 below the predicted line radiation, and therefore, even in the absence of a fast detector, will not mask this radiation.

This Letter has shown that the essential cooling rate of a heavy metal, together with the loss-modified thermal conductivity, allows an x-ray pulse to replicate a laser pulse on a femtosecond time scale; and to achieve such an x-ray pulse, the density of the heavy metal must be reduced to a level commensurate with the absorbed laser energy. For a 10^{-13}-s, 10^{12}-W (peak) laser driver,[15] and 5% laser absorption (inverse bremsstrahlung at 1 keV), the method outlined allows the generation of femtosecond x-ray pulses with a peak power of $\simeq5\times10^6$ W. At 10 Hz this will produce a point source of 3.5-Å x-rays with an average power of 4 μW ($\simeq10^{10}$ phonons/s), thereby allowing x-ray diffraction on a femtosecond time scale.

The authors gratefully acknowledge helpful discussions with Roger Falcone, John Macklin, and Atac Imamoglu. This work was supported by the U.S. Air Force Office of Scientific Research, the U.S. Army

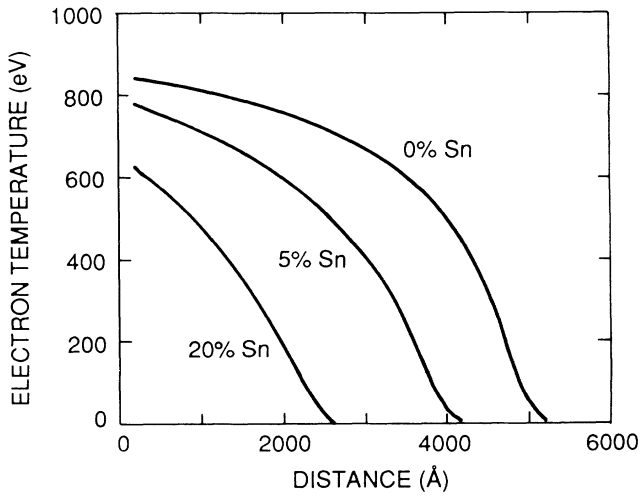

FIG. 2. Electron temperature vs distance at an absorbed energy of 1 kJ/cm^2, for different values of tin density. The profiles are evaluated 50 fs after the peak of the laser pulse.

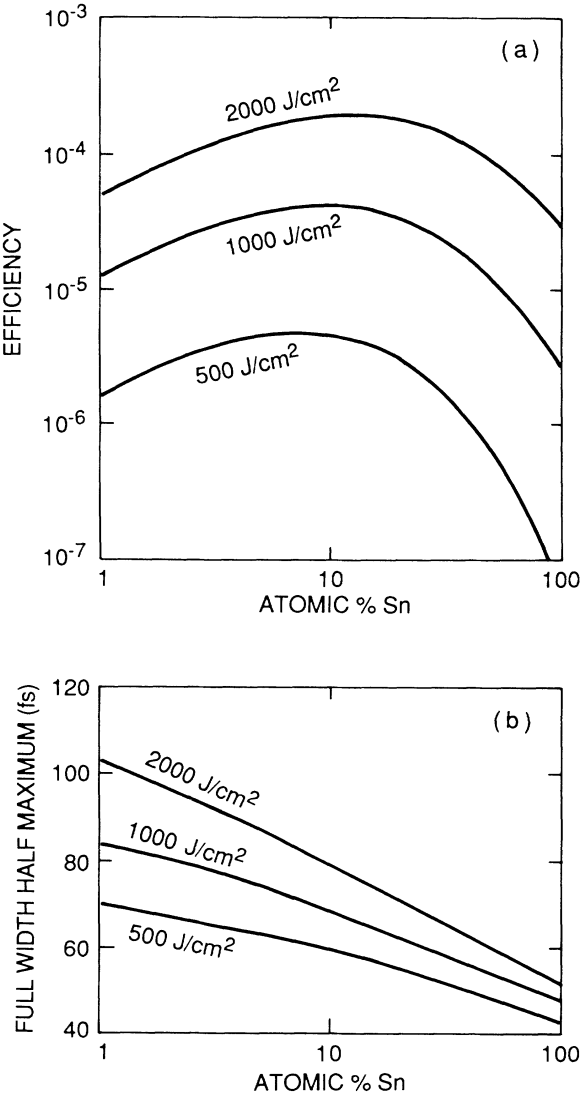

FIG. 3. (a) X-ray peak power conversion efficiency ($\lambda=3.6$ Å) as a function of percent tin. (b) X-ray pulse width for a 100-fs laser pulse.

Research Office, and the U.S. Office of Naval Research.

[1]E. J. McGuire, Phys. Rev. A **5**, 1043 (1972).

[2]E. J. McGuire, Phys. Rev. A **3**, 587 (1971).

[3]R. W. Falcone and M. M. Murnane, in *Short Wavelength Coherent Radiation: Generation and Applications,* edited by D. T. Attwood and J. Bokor, AIP Conference Proceedings No. 147 (American Institute of Physics, New York, 1986), pp. 81–85.

[4]O. R. Wood, II, W. T. Silfvast, H. W. K. Tom, W. H. Knox, R. L. Fork, C. H. Brito-Cruz, P. J. Maloney, and C. V. Shank, J. Opt. Soc. Am. B **13**, 24 (1987).

[5]D. Kuehlke, V. Herpers, and D. Von der Linde, Appl. Phys. Lett. **50**, 1785 (1987).

[6]D. W. Phillion and C. J. Hailey, Phys. Rev. A **34**, 4886 (1986).

[7]D. G. Stearns, O. L. Landen, E. M. Campbell, and J. Scofield, Phys. Rev. A **37**, 1684 (1988).

[8]Noboru Nakano and Hiroto Kuroda, Phys. Rev. A **35**, 4719 (1987).

[9]L. Spitzer, Jr., *Physics of Fully Ionized Gases* (Interscience, New York, 1982).

[10]H. A. Bethe, *Intermediate Quantum Mechanics,* (Benjamin, New York, 1964), p. 177.

[11]D. Mosher, Phys. Rev. A **10**, 2330 (1974).

[12]T. A. Carlson, C. W. Nestor, Jr., N. Wasserman, and J. D. McDowell, At. Data **2**, 63 (1970).

[13]T. A. Carlson, W. E. Hunt, and M. O. Krause, Phys. Rev. **151**, 41 (1966).

[14]A. Caruso and R. Gratton, Plasma Phys. **11**, 839 (1969).

[15]M. Pessot, P. Maine, and G. Mourou, Opt. Commun. **62**, 419 (1987).